Int. J. Solids Structures, 1971, Vol. 7, pp. 1237 to 1259. Pergamon Press. Printed in Great Britain

# BUCKLING AND INITIAL POST-BUCKLING BEHAVIOR OF CLAMPED SHALLOW SPHERICAL SANDWICH SHELLS

NURI AKKAŞ† and NELSON R. BAULD, JR.‡

Engineering Mechanics Department, Clemson University, Clemson, S.C.

**Abstract**—This paper presents the development of a set of nonlinear differential equations that are suitable for the analysis of the buckling and initial post-buckling behavior of thin shallow spherical sandwich shells under axisymmetrical loads. The boundary value problems associated with the axisymmetrical, asymmetrical and initial post-buckling behaviors for clamped shallow spherical sandwich shells under certain axisymmetrical loads are developed also. Finally, numerical results of the buckling and initial post-buckling behavior of the clamped shallow spherical sandwich shell under pressures that are distributed uniformly over the entire reference surface of the shell are studied for face sheets of the same material and equal thicknesses. The numerical results show that the buckling and initial post-buckling behavior for the sandwich cap is very similar to that for the classical homogeneous cap.

## INTRODUCTION

THE principal purpose of this paper is to present a sequence of boundary value problems that are relevant to the analysis of the buckling and initial post-buckling behavior of clamped shallow spherical sandwich shells with dissimilar face sheets under certain axisymmetrical loads. A secondary purpose is the presentation of numerical results obtained via the foregoing boundary value problems for the clamped shallow spherical sandwich shell under pressures that are distributed uniformly over the entire reference surface of the shell.

The theoretical treatment employed in this study is essentially a perturbation technique proposed by Koiter [1] and which was transcribed into a form suitable for application to the clamped shallow spherical homogeneous shell by Fitch [2]. The buckling and initial post-buckling behavior of clamped shallow spherical homogeneous shells under various types of loads has been studied extensively in recent years [2–8]. It has been suggested, in the literature, that the clamped shallow spherical homogeneous shell can be regarded as a reasonable approximation of the substructure which supports the ablation material of the heat shield on space vehicles. Since this substructure is likely to be a sandwich construction it is clear that the buckling and initial post-buckling analyses of clamped shallow spherical sandwich shells have significant practical implications. The authors of this paper were unable to uncover any previous studies of this nature relative to the sandwich cap.

† Graduate Research Assistant.
‡ Professor.

## MATHEMATICAL MODEL

The mathematical model used in this investigation to study the buckling and initial post-buckling behavior of clamped shallow spherical sandwich shells under axisymmetric loads to be described in the sequel is obtained via the variational principle of stationary potential energy.

*Face sheets*

The isotropic face sheets may be of unequal thicknesses and of different materials; however, the Poisson ratios for the two face sheets are assumed to be equal. Moreover, the middle surface displacements are assumed to satisfy the strain–displacement relations

$$\left.\begin{aligned} e_{ri} &= U_i' + \frac{r}{R} W_i' + \tfrac{1}{2}(W_i')^2, \\ e_{\varphi i} &= \frac{1}{r} U_i + \frac{1}{r} \dot{V}_i + \frac{1}{2}\left(\frac{1}{r} \dot{W}_i\right)^2, \\ e_{r\varphi i} &= \frac{1}{2}\left[\frac{1}{r} \dot{U}_i - \frac{1}{r} V_i + V_i' + \frac{1}{R} \dot{W}_i + \frac{1}{r} \dot{W}_i W_i'\right], \end{aligned}\right\} \tag{1}$$

and the displacements are assumed to vary through thickness according to the relations

$$\left.\begin{aligned} \bar{U}_i &= U_i - zW_i', \\ \bar{V}_i &= V_i - \frac{z}{r} \dot{W}_i, \\ \bar{W}_i &= W_i. \end{aligned}\right\} \tag{2}$$

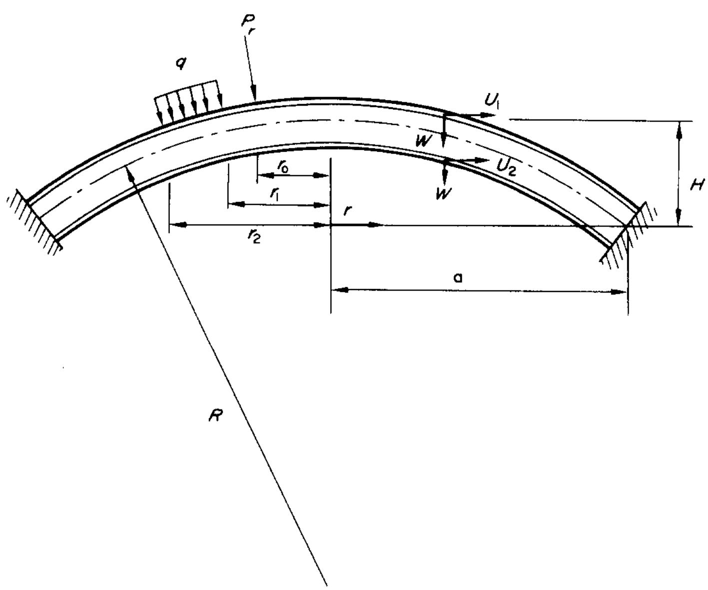


FIG. 1. Geometry of a clamped sandwich spherical cap.

In equation (1) $R$ denotes the radius of curvature of the composite cap as shown in Fig. (1). A remark concerning the notation employed in this paper is in order. The subscript $i$ signifies the face sheet under consideration while the operations of differentiation are denoted by

$$(\ )' \equiv \frac{\partial}{\partial r}(\ ), \qquad (\dot{\ }) \equiv \dot{(\ )} \equiv \frac{\partial}{\partial \varphi}(\ ),$$

and

$$\nabla^2(\ \ ) \equiv (\ \ )'' + \frac{1}{r}(\ \ )' + \frac{1}{r^2}(\ddot{\ \ }).$$

Other subscripts, where they appear, are to be interpreted in the manner of elasticity theory.

The change in curvature relations are given by

$$\left.\begin{aligned} \kappa_{ri} &= -W_i'', \\ \kappa_{\varphi i} &= -\frac{1}{r^2}\ddot{W}_i - \frac{1}{r}W_i', \\ \kappa_{r\varphi i} &= -\left(\frac{1}{r}\dot{W}_i\right)'. \end{aligned}\right\} \tag{3}$$

The first order variations in the internal virtual work of the face sheets and the external virtual work of pressure are respectively,

$$\delta H_f = \sum_{i=1}^{2}\int_A \{N_{ri}\delta e_{ri} + N_{\varphi i}\delta e_{\varphi i} + 2N_{r\varphi i}\delta e_{r\varphi i} + M_{ri}\delta\kappa_{ri} + M_{\varphi i}\delta\kappa_{\varphi i} + 2M_{r\varphi i}\delta\kappa_{r\varphi i}\} r\,\mathrm{d}\varphi\,\mathrm{d}r, \tag{4}$$

$$\delta\Omega = \sum_{i=1}^{2}\int_A \{q_i\delta W_i\} r\,\mathrm{d}\varphi\,\mathrm{d}r. \tag{5}$$

Here $q_i$ signifies the transverse distributed load that is applied to the middle surface of the $i$th face sheet and $A$ is the projected area of the shallow shell.

The first order variation in the external virtual work of the edge loads, which are distinguished herein by asterisks, is

$$\begin{aligned} \delta\Omega_i^* = &-\int_C rN_{ri}^*\delta U_i\,\mathrm{d}\varphi - \int_C rN_{r\varphi i}^*\delta V_i\,\mathrm{d}\varphi + \int_C N_{\varphi i}^*\delta V_i\,\mathrm{d}r + \int_C N_{\varphi ri}^*\delta U_i\,\mathrm{d}r \\ &-\int_C rQ_{ri}^*\delta W_i\,\mathrm{d}\varphi + \int_C Q_{\varphi i}^*\delta W_i\,\mathrm{d}r + \int_C rM_{ri}^*\delta W_i'\,\mathrm{d}\varphi \\ &+\int_C rM_{r\varphi i}^*\left(\frac{1}{r}\,\delta\dot{W}_i\right)\mathrm{d}\varphi - \int_C M_{\varphi i}^*\left(\frac{1}{r}\,\delta\dot{W}_i\right)\mathrm{d}r - \int_C M_{\varphi ri}^*\,\delta W_i'\,\mathrm{d}r, \end{aligned} \tag{6}$$

where $C$ signifies the bounding contour of the shell.

The membrane stress resultant–strain relations are

$$\left.\begin{aligned} B_i(1-\nu^2)e_{ri} &= N_{ri} - \nu N_{\varphi i}, \\ B_i(1-\nu^2)e_{\varphi i} &= N_{\varphi i} - \nu N_{ri}, \\ B_i(1-\nu)e_{r\varphi i} &= N_{r\varphi i}, \text{ where } B_i = E_i t_i/(1-\nu^2). \end{aligned}\right\} \tag{7}$$

Here, $E_i$ and $t_i$ denote Young's modulus and the thickness of the $i$th face sheet respectively. Poisson's ratio is denoted by $\nu$. Finally, the moment stress resultants are expressed in terms of the changes in curvatures by the relations

$$\left.\begin{aligned} M_{ri} &= D_i(\kappa_{ri} + \nu\kappa_{\varphi i}),\\ M_{\varphi i} &= D_i(\kappa_{\varphi i} + \nu\kappa_{ri}),\\ M_{r\varphi i} &= D_i(1-\nu)\kappa_{r\varphi i}, \quad \text{where} \quad D_i = E_i t_i^3/[12(1-\nu^2)]. \end{aligned}\right\} \tag{8}$$

*Core*

The core material is assumed to be an isotropic homogeneous continuum capable of transmitting transverse shearing forces only. Consequently, the rigid core theory of sandwich construction is adopted. Moreover, the meridional and circumferential displacements in the region occupied by the core material are assumed to vary linearly through the core thickness, accordingly, in view of relations (2) (with $W_1 = W_2 = W$) and Fig. 3, these dis-

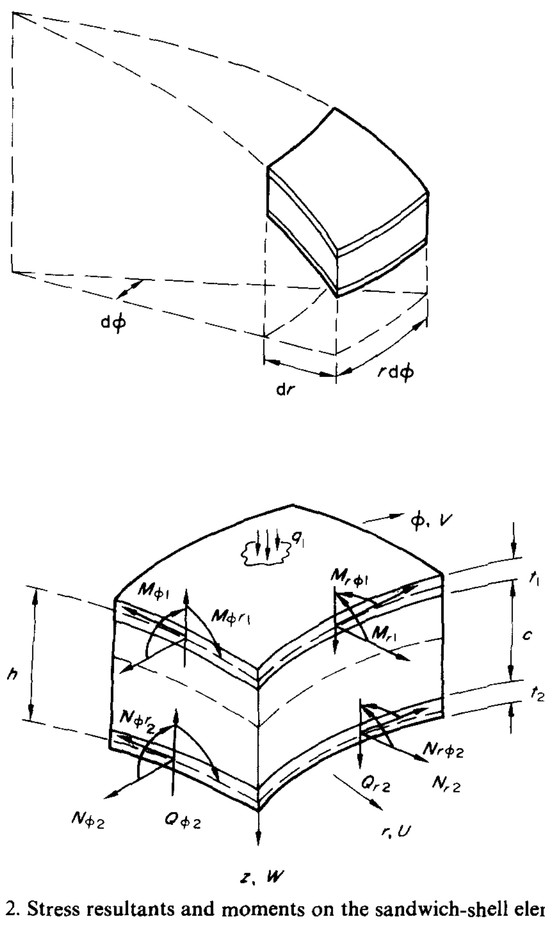


FIG. 2. Stress resultants and moments on the sandwich-shell element.

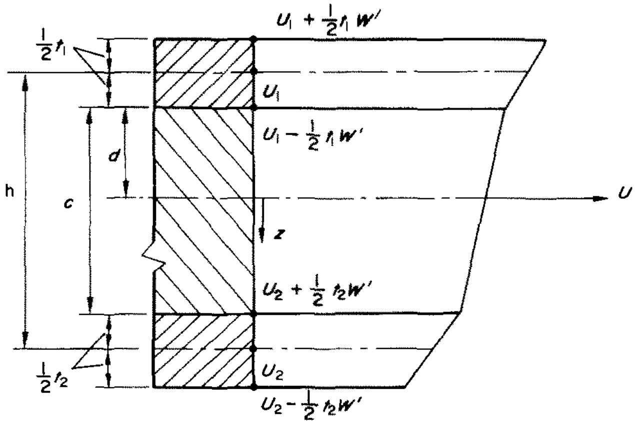


FIG. 3. Plot of $U$ displacements through the thickness of the shell.

placements can be written

$$\left.\begin{aligned} U_C &= \left(U_1 - \frac{t_1}{2} W'\right) - \frac{d+z}{c}\left[(U_1 - U_2) - \frac{t_1+t_2}{2} W'\right], \\ V_C &= \left(V_1 - \frac{t_1}{2r} \dot{W}\right) - \frac{d+z}{c}\left[(V_1 - V_2) - \frac{t_1+t_2}{2r} \dot{W}\right]. \end{aligned}\right\} \tag{9}$$

In expression (9), $c$ denotes the thickness of the core material and $d$ is the distance from the reference surface of the composite shell to the interface between the core material and the face-sheet signified by the numeral 1 (Fig. 3). The transverse shearing strains associated with the core material are calculated from the basic formulas

$$\gamma_{rz} = \frac{\partial U_C}{\partial z} + W', \qquad \gamma_{\varphi z} = \frac{\partial V_C}{\partial z} + \frac{1}{r}\dot{W}. \tag{10}$$

Equations (9) and (10) lead to the formulas

$$\left.\begin{aligned} \gamma_{rz} &= -\frac{h}{c}(\alpha - W'), \\ \gamma_{\varphi z} &= -\frac{h}{c}\left(\beta - \frac{1}{r}\dot{W}\right), \end{aligned}\right\} \tag{11}$$

where

$$\alpha = \frac{U_1 - U_2}{h}, \qquad \beta = \frac{V_1 - V_2}{h}, \qquad h = c + \frac{t_1 + t_2}{2} \tag{12}$$

The first order variation in the internal virtual work of the core material, whose transverse shearing modulus is denoted by $G_c$, is

$$\delta H_c = G_c c \int_A \{\gamma_{rz}\delta\gamma_{rz} + \gamma_{\varphi z}\delta\gamma_{\varphi z}\} r \, \mathrm{d}\varphi \, \mathrm{d}r. \tag{13}$$

*Equilibrium equations—boundary conditions*

The equilibrium configurations of a conservative mechanical system are characterized by a stationary value of the total potential energy of the system. Consequently, after repeated integrations by parts, equations (4)–(6) and (13), with the aid of equations (1), (3) and (11) yield (with $W_1 = W_2 = W$)

$$\delta V = \int_A \sum_{i=1}^{2} \Bigg\{ [-(rN_{ri})' + N_{\varphi i} - \dot{N}_{r\varphi i}]\delta U_i + [-\dot{N}_{\varphi i} - N_{r\varphi i} - (rN_{r\varphi i})']\delta V_i$$
$$+ \Bigg[ -\frac{(r^2 N_{ri})'}{R} - (rN_{ri}W')' - \frac{1}{r}\dot{\overline{(N_{\varphi i}\dot{W})}} - \frac{r\dot{N}_{r\varphi i}}{R} - (N_{r\varphi i}\dot{W})' - \dot{\overline{(N_{r\varphi i}W')}} - (rM_{ri})''$$
$$- \frac{1}{r}\ddot{M}_{\varphi i} + M'_{\varphi i} - 2\dot{M}'_{r\varphi i} - \frac{2}{r}\dot{M}_{r\varphi i} - rq_i \Bigg]\delta W \Bigg\} \mathrm{d}r\,\mathrm{d}\varphi$$
$$+ \frac{G_c h^2}{c}\int_A \Bigg\{ r(\alpha - W')\delta\alpha + r\left(\beta - \frac{1}{r}\dot{W}\right)\delta\beta + [(r\alpha)' + \dot{\beta} - r\nabla^2 W]\delta W \Bigg\}\,\mathrm{d}r\,\mathrm{d}\varphi$$
$$- \int_C \sum_{i=1}^{2} \Bigg\{ (N^*_{ri} - N_{ri})\delta U_i r\,\mathrm{d}\varphi - (N^*_{\varphi ri} - N_{\varphi ri})\delta U_i\,\mathrm{d}r - (N^*_{\varphi i} - N_{\varphi i})\delta V_i\,\mathrm{d}r$$
$$+ (N^*_{r\varphi i} - N_{r\varphi i})\delta V_i r\,\mathrm{d}\varphi - (M^*_{ri} - M_{ri})\delta W' r\,\mathrm{d}\varphi$$
$$+ (M^*_{\varphi i} - M_{\varphi i})\frac{1}{r}\delta\dot{W}\,\mathrm{d}r + \Bigg[ Q^*_{ri} + \frac{1}{r}\dot{M}^*_{r\varphi i} - \frac{r}{R}N_{ri} - N_{ri}W'$$
$$- \frac{1}{r}N_{r\varphi i}\dot{W} - \frac{1}{r}(rM_{ri})' + \frac{1}{r}M_{\varphi i} - \frac{2}{r}\dot{M}_{r\varphi i} + \frac{G_c h^2}{c}(\alpha - W') \Bigg]\delta W r\,\mathrm{d}\varphi$$
$$- \Bigg[ Q^*_{\varphi i} + M^{*\prime}_{\varphi ri} - \frac{1}{r}N_{\varphi i}\dot{W} + \frac{r}{R}N_{r\varphi i} - N_{r\varphi i}W' - \frac{1}{r}\dot{M}_{\varphi i} - 2M'_{r\varphi i} - \frac{2}{r}M_{r\varphi i}$$
$$+ \frac{G_c h^2}{c}\left(\beta - \frac{1}{r}\dot{W}\right) \Bigg]\,\delta W\,\mathrm{d}r \Bigg\} + 2\sum_{i=1}^{2}(M^*_{r\varphi i} - M_{r\varphi i})\delta W \Bigg|_{\varphi_1}^{\varphi_2}\Bigg|_{r_1}^{r_2} = 0. \quad (14)$$

The summation signs appearing in equation (14) can be removed by making appropriate transformations in variables. Thus by setting

$$\bar{U} = \frac{B_1 U_1 + B_2 U_2}{B_1 + B_2}, \qquad \bar{V} = \frac{B_1 V_1 + B_2 V_2}{B_1 + B_2} \quad (15)$$

and observing the definitions (12) there is obtained

$$\left.\begin{aligned} U_1 &= \bar{U} + \frac{B_2 h}{B_1 + B_2}\alpha, \qquad & U_2 &= \bar{U} - \frac{B_1 h}{B_1 + B_2}\alpha \\ V_1 &= \bar{V} + \frac{B_2 h}{B_1 + B_2}\beta, \qquad & V_2 &= \bar{V} - \frac{B_1 h}{B_1 + B_2}\beta. \end{aligned}\right\} \quad (16)$$

Substitution of equations (16) into equation (14), and subsequent use of the following transformations,

$$\left.\begin{array}{lll} N_r = N_{r1}+N_{r2}, & M_r = M_{r1}+M_{r2}, & Q_r = Q_{r1}+Q_{r2}, \\ N_\varphi = N_{\varphi 1}+N_{\varphi 2}, & M_\varphi = M_{\varphi 1}+M_{\varphi 2}, & Q_\varphi = Q_{\varphi 1}+Q_{\varphi 2}, \\ N_{r\varphi} = N_{r\varphi 1}+N_{r\varphi 2}, & M_{r\varphi} = M_{r\varphi 1}+M_{r\varphi 2}, & q = q_1+q_2, \end{array}\right\} \tag{17}$$

yields

$$\begin{aligned}
&-\int_A \{P_1\delta\bar{U}+P_2\delta\bar{V}+P_3\delta W+P_4\delta\alpha+P_5\delta\beta\}\,\mathrm{d}\varphi\,\mathrm{d}r \\
&-\int_C (N_r^*-N_r)\delta\bar{U}r\,\mathrm{d}\varphi+\int_C (N_{\varphi r}^*-N_{\varphi r})\delta\bar{U}r\,\mathrm{d}\varphi+\int_C (N_\varphi^*-N_\varphi)\delta\bar{V}\,\mathrm{d}r \\
&-\int_C (N_{r\varphi}^*-N_{r\varphi})\delta\bar{V}\,\mathrm{d}r-\int_C (V_r^*-V_r)\delta Wr\,\mathrm{d}\varphi+\int_C (V_\varphi^*-V_\varphi)\delta W\,\mathrm{d}r \\
&+\int_C (M_r^*-M_r)\delta W'r\,\mathrm{d}\varphi-\int_C (M_\varphi^*-M_\varphi)\frac{1}{r}\,\delta\dot{W}\,\mathrm{d}r \\
&+2(M_{r\varphi}^*-M_{r\varphi})\delta W\Big|_{\varphi_1}^{\varphi_2}\Big|_{r_1}^{r_2} \\
&-\int_C \frac{h}{B_1+B_2}\{(B_2N_{r1}^*-B_1N_{r2}^*)-(B_2N_{r1}-B_1N_{r2})\}\delta\alpha r\,\mathrm{d}\varphi \\
&+\int_C \frac{h}{B_1+B_2}\{(B_2N_{\varphi r1}^*-B_1N_{\varphi r2}^*)-(B_2N_{\varphi r1}-B_1N_{\varphi r2})\}\delta\alpha\,\mathrm{d}r \\
&+\int_C \frac{h}{B_1+B_2}\{(B_2N_{\varphi 1}^*-B_1N_{\varphi 2}^*)-(B_2N_{\varphi 1}-B_1N_{\varphi 2})\}\delta\beta\,\mathrm{d}r \\
&\int_C \frac{h}{B_1+B_2}\{(B_2N_{r\varphi 1}^*-B_1N_{r\varphi 2}^*)-(B_2N_{r\varphi 1}-B_1N_{r\varphi 2})\}\delta\beta r\,\mathrm{d}\varphi = 0.
\end{aligned} \tag{18}$$

The quantities $P_i$ appearing in equation (18) are defined by the formulas

$$\left.\begin{aligned}
P_1 &= (rN_r)'-N_\varphi+\dot{N}_{r\varphi}, \\
P_2 &= \dot{N}_\varphi+N_{r\varphi}+(rN_{r\varphi})', \\
P_3 &= \frac{(r^2N_r)'}{R}+(rN_rW')'+\frac{1}{r}\overline{N_\varphi\dot{W}}^{\cdot}+\frac{r}{R}\dot{N}_{r\varphi}+(N_{r\varphi}\dot{W})'+(\overline{N_{r\varphi}W'})^{\cdot} \\
&\quad+(rM_r)''+\frac{1}{r}\ddot{M}_\varphi-M_\varphi'+2\dot{M}_{r\varphi}'+\frac{2}{r}\dot{M}_{r\varphi}+rq-\frac{G_ch^2}{c}[(r\alpha)'+\dot{\beta}-r\nabla^2W], \\
P_4 &= \frac{B_2h}{B_1+B_2}[(rN_{r1})'-N_{\varphi 1}+\dot{N}_{r\varphi 1}]-\frac{B_1h}{B_1+B_2}[(rN_{r2})'-N_{\varphi 2}+\dot{N}_{r\varphi 2}]-\frac{G_ch^2}{c}\,r(\alpha-W'), \\
P_5 &= \frac{B_2h}{B_1+B_2}[\dot{N}_{\varphi 1}+N_{r\varphi 1}+(rN_{r\varphi 1})']-\frac{B_1h}{B_1+B_2}[\dot{N}_{\varphi 2}+N_{r\varphi 2}+(rN_{r\varphi 2})']-\frac{G_ch^2}{c} \\
&\quad\times r\left(\beta-\frac{1}{r}\,\dot{W}\right).
\end{aligned}\right\} \tag{19}$$

Likewise, the generalized transverse shearing forces appearing there are given by

$$\left.\begin{aligned} V_r^* &= -(D_1+D_2)\left[(\nabla^2 W)' + \frac{(1-\nu)}{r}\left(\frac{1}{r}\ddot{W}\right)'\right] + \frac{r}{R}N_r + N_r W' \\ &\quad + \frac{1}{r}N_{r\varphi}\dot{W} - \frac{G_c h^2}{c}(\alpha - W'), \\ V_\varphi^* &= -(D_1+D_2)\left[\frac{1}{r}\dot{\overline{(\nabla^2 W)}} + (1-\nu)\left(\frac{1}{r}\dot{W}\right)''\right] \\ &\quad - \frac{r}{R}N_{r\varphi} + \frac{1}{r}N_\varphi \dot{W} + N_{r\varphi}W' - \frac{G_c h^2}{c}\left(\beta - \frac{1}{r}\dot{W}\right). \end{aligned}\right\} \tag{20}$$

The equilibrium equations for the shallow spherical sandwich shell result from equating $P_1$–$P_5$ in equation (19) to zero. To complete the theory the transverse shearing forces are given by

$$\left.\begin{aligned} Q_r &= -(D_1+D_2)(\nabla^2 W)' + \frac{r}{R}N_r + N_r W' + \frac{1}{r}N_{r\varphi}\dot{W} - \frac{G_c h^2}{c}(\alpha - W'), \\ Q_\varphi &= -(D_1+D_2)\frac{1}{r}\dot{\overline{(\nabla^2 W)}} - \frac{r}{R}N_{r\varphi} + \frac{1}{r}N_\varphi \dot{W} + N_{r\varphi}W' - \frac{G_c h^2}{c}\left(\beta - \frac{1}{r}\dot{W}\right). \end{aligned}\right\} \tag{21}$$

*Final form for the equilibrium equations*

The first two of equations (19) are satisfied by the Airy stress function $F(r, \varphi)$ defined by the relations

$$\left.\begin{aligned} N_r &= \frac{1}{r}F' + \frac{1}{r^2}\ddot{F}, \\ N_\varphi &= F'', \\ N_{r\varphi} &= -\frac{1}{r}\dot{F}' + \frac{1}{r^2}\dot{F}. \end{aligned}\right\} \tag{22}$$

The third of equations (19) can now be written, with the use of equations (3), (8) and (22), in the form

$$\begin{aligned} (D_1+D_2)\nabla^4 W &= q + \frac{1}{R}\nabla^2 F - 2\left(\frac{1}{r}\dot{F}' - \frac{1}{r^2}\dot{F}\right)\left(\frac{1}{r}\dot{W}' - \frac{1}{r^2}\dot{W}\right) + F''\left(\frac{1}{r^2}\ddot{W} + \frac{1}{r}W'\right) \\ &\quad + W''\left(\frac{1}{r}F' + \frac{1}{r^2}\ddot{F}\right) - \frac{G_c h^2}{c}\left\{\frac{1}{r}[(r\alpha)' + \dot{\beta}] - \nabla^2 W\right\}. \end{aligned} \tag{23}$$

A compatibility equation can be obtained for each face sheet by eliminating the meridional and circumferential components of displacement from the strain–displacement relations (1), accordingly,

$$\frac{1}{r}(re_{\varphi i})'' - \frac{1}{r}e'_{ri} - \frac{2}{r^2}(r\dot{e}_{r\varphi i})' + \frac{1}{r^2}\ddot{e}_{ri} = -\frac{1}{R}\nabla^2 W + \left(\frac{1}{r}\dot{W}' - \frac{1}{r^2}\dot{W}\right)^2 - W''\left(\frac{1}{r}W' + \frac{1}{r^2}\ddot{W}\right).$$

Writing the foregoing equation for each face sheet, making use of equations (7) and (22), and adding the results yields

$$\nabla^4 F = (B_1+B_2)(1-\nu^2)\left[-\frac{1}{R}\nabla^2 W + \left(\frac{1}{r}\dot{W}' - \frac{1}{r^2}\dot{W}\right)^2 - W''\left(\frac{1}{r}W' + \frac{1}{r^2}\ddot{W}\right)\right]. \tag{24}$$

Finally, using equations (1) and (7) and the definitions for $\alpha$ and $\beta$ given by equations (12), the last two of equations (19) can be written in the form

$$\frac{1-\nu}{2}\nabla^2\alpha + \frac{1+\nu}{2}\left(\alpha'' + \frac{1}{r}\alpha' + \frac{1}{r}\dot{\beta}'\right) - \frac{1}{r^2}\alpha - \frac{3-\nu}{2r^2}\dot{\beta} - \frac{G_c(B_1+B_2)}{cB_1B_2}(\alpha - W') = 0, \tag{25}$$

$$\frac{1-\nu}{2}\nabla^2\beta + \frac{1+\nu}{2}\left(\frac{1}{r}\dot{\alpha}' + \frac{1}{r^2}\ddot{\beta}\right) + \frac{3-\nu}{2r^2}\dot{\alpha} - \frac{1-\nu}{2r^2}\beta - \frac{G_c(B_1+B_2)}{cB_1B_2}\left(\beta - \frac{1}{r}\dot{W}\right) = 0. \tag{26}$$

Equations (23)–(26) constitute the mathematical description of the moderately large deflections of shallow spherical sandwich shells consistent with the rigid core theory of sandwich shells. In the sequel these equations will be the basis for the study of the buckling and initial post-buckling behavior of clamped shallow spherical sandwich shells under axisymmetric transverse loadings.

## BUCKLING AND INITIAL POST-BUCKLING ANALYSIS

### *Basic equations*

The buckling and initial post-buckling behavior of thin clamped shallow spherical sandwich shells under axisymmetric loads of the types listed below can be studied conveniently via the non-dimensional form of the system of equations (23)–(26):

$$\begin{aligned}\nabla^4 w = \Gamma + \nabla^2 f - 2\left(\frac{1}{x}\dot{f}' - \frac{1}{x^2}\dot{f}\right)\left(\frac{1}{x}\dot{w}' - \frac{1}{x^2}\dot{w}\right) + \left(\frac{1}{x^2}\ddot{w} + \frac{1}{x}w'\right)f''\\ + \left(\frac{1}{x}f' + \frac{1}{x^2}\ddot{f}\right)w'' - \eta\left\{\frac{1}{x}[(x\bar{\alpha})' + \dot{\bar{\beta}}] - \nabla^2 w\right\},\end{aligned} \tag{27}$$

$$\nabla^4 f = -\nabla^2 w + \left(\frac{1}{x}\dot{w}' - \frac{1}{x^2}\dot{w}\right)^2 - \left(\frac{1}{x}w' + \frac{1}{x^2}\ddot{w}\right)w'', \tag{28}$$

$$\frac{1-\nu}{2}\nabla^2\bar{\alpha} + \frac{1+\nu}{2}\left(\bar{\alpha}'' + \frac{1}{x}\bar{\alpha}' + \frac{1}{x}\dot{\bar{\beta}}'\right) - \frac{1}{x^2}\bar{\alpha} - \frac{3-\nu}{2x^2}\dot{\bar{\beta}} - \Lambda(\bar{\alpha} - w') = 0, \tag{29}$$

$$\frac{1-\nu}{2}\nabla^2\bar{\beta} + \frac{1+\nu}{2}\left(\frac{1}{x}\dot{\bar{\alpha}}' + \frac{1}{x^2}\ddot{\bar{\beta}}\right) + \frac{3-\nu}{2x^2}\dot{\bar{\alpha}} - \frac{1-\nu}{2x^2}\bar{\beta} - \Lambda\left(\bar{\beta} - \frac{1}{x}\dot{w}\right) = 0, \tag{30}$$

with boundary conditions at the clamped edge ($x = \lambda$)

$$w = 0, \tag{31}$$

$$w' = 0, \tag{32}$$

$$f'' - \frac{\nu}{\lambda}f' - \frac{\nu}{\lambda^2}\ddot{f} = 0, \tag{33}$$

$$\lambda\left(f'' - \frac{\nu}{x}f' - \frac{\nu}{x^2}\mathring{f}\right)' - \frac{1}{\lambda}f' - \frac{1}{\lambda^2}\mathring{f} + \nu f'' + 2(1+\nu)\left(\frac{1}{x}\mathring{f}\right)' = 0, \tag{34}$$

$$\bar{\alpha} = 0, \tag{35}$$

$$\bar{\beta} = 0. \tag{36}$$

The non-dimensional quantities appearing in equations (27)–(36) are related to the corresponding physical quantities through the relations

$$\left.\begin{aligned}
&\lambda = 2[3(1-\nu^2)]^{\frac{1}{4}}\left(\frac{H}{t^*}\right)^{\frac{1}{2}}, \qquad (t^*)^2 = \frac{E_1 t_1^3 + E_2 t_2^3}{E_1 t_1 + E_2 t_2},\\
&x = \frac{\lambda}{a} r, \qquad \alpha = \frac{2H}{\lambda a}\bar{\alpha}, \qquad \beta = \frac{2H}{\lambda a}\bar{\beta},\\
&w = \frac{\lambda^2}{2H} W, \qquad f = \frac{\lambda^4}{4H^2(E_1 t_1 + E_2 t_2)} F,\\
&\mu = \frac{t_1 + t_2}{2c}, \qquad \eta = \frac{G_c c}{E_1 t_1 + E_2 t_2}\left(\frac{a}{H}\right)^2 \frac{\lambda^2 (1+\mu)^2}{4}, \qquad \Lambda = \frac{G_c(B_1 + B_2)}{cB_1 B_2}\left(\frac{a}{\lambda}\right)^2.
\end{aligned}\right\} \tag{37}$$

In the foregoing expressions $a$, $R$ and $H$ are, respectively, the base plane radius, radius of curvature of the sandwich cap and apex rise referred to the reference surface of the composite cap. The thicknesses of the face sheets and the core material are denoted by $t_1$, $t_2$ and $c$, respectively. Young's moduli for the face sheets are denoted by $E_1$ and $E_2$, the transverse shearing modulus of the core by $G_c$ and the Poisson ratio by $\nu$ (Poisson's ratios for the two face sheets are assumed to be equal). The quantities $w$, $f$, $\bar{\alpha}$, $\bar{\beta}$ are the non-dimensional transverse deflection, Airy stress function and shear angles, respectively; and $W$, $F$, $\alpha$, $\beta$ are the corresponding physical quantities. Finally, the delta operator has the same meaning as before with $r$ replaced by $x$, and $\Gamma$ represents the non-dimensional axisymmetric load under consideration.

The boundary value problem described by equations (27)–(36) is completed by assigning appropriate regularity conditions at the apex. The conditions will be prescribed as the need arises.

*Nondimensional axisymmetric loads*

The axisymmetric loads considered in this investigation are defined by the relations

$$\Gamma = \left\{\begin{array}{lll}
p\dfrac{\delta(x-x_0)}{x}, & p = \dfrac{PR}{2\pi(D_1 + D_2)}, & P = 2\pi r_0 P_r, \text{ (ring load)}\\[2ex]
4p[h(x-x_1) - h(x-x_2)], & p = \dfrac{a^4\lambda^2 q}{32(E_1 t_1 + E_2 t_2)H^3}, \text{ (band load)} &
\end{array}\right\} \tag{38}$$

where $x_0$, $x_1$, $x_2$ are the nondimensional forms of $r_0$, $r_1$, $r_2$, respectively, which are shown in Fig. 1.

The Dirac delta is defined by the relations

$$\delta(x-x_0) = \begin{cases} 0 & x \neq x_0 \\ \infty & x = x_0 \end{cases} \quad \text{and} \quad \int_0^x \delta(\xi-x_0)\,\mathrm{d}\xi = h(x-x_0) \tag{39}$$

and the Heaviside function is defined by

$$h(x-x_i) = \begin{cases} 0 & x < x_i \\ 1 & x \geq x_i, \qquad (i = 1, 2). \end{cases} \tag{40}$$

It is observed that the concentrated force applied at the apex is included as a limiting case of the ring load (let $x_0 \to 0$ while maintaining $P$ constant) and the important cases of centrally distributed pressures and pressures distributed uniformly over the entire cap are included as special cases of the band load.

When the axisymmetric form of equations (27)–(36) is considered it is found that equations (27) and (28) can be integrated once with respect to $x$ directly. Consequently, the form of $\Gamma$ to be used in the axisymmetric equation (43) is denoted by $\Gamma^*$ and is given by

$$\Gamma^* = \begin{cases} ph(x-x_0), & \text{(ring load)} \\ 2p(x_2^2-x_1^2)Z(x), & \text{(band load)} \end{cases} \tag{41}$$

where

$$Z(x) = \begin{cases} 0 & x \leq x_1 \\ \dfrac{x^2-x_1^2}{x_2^2-x_1^2} & x_1 < x < x_2 \\ 1 & x \geq x_2. \end{cases} \tag{42}$$

*Axisymmetrical behavior*

The boundary value problem governing the axisymmetrical deformations of the clamped shallow spherical sandwich cap under the axisymmetrical loads described reduces to

$$(x\Theta')' - \frac{1}{x}\Theta + x\Phi - \eta x(\alpha_0+\Theta) = -\Gamma^* + \Theta\Phi, \tag{43}$$

$$(x\Phi')' - \frac{1}{x}\Phi - x\Theta = -\tfrac{1}{2}\Theta^2, \tag{44}$$

$$\nabla^2\alpha_0 - \frac{1}{x^2}\alpha_0 - \Lambda(\alpha_0+\Theta) = 0, \tag{45}$$

$$\Theta(\lambda) = 0, \tag{46}$$

$$\lambda\Phi'(\lambda) - \nu\Phi(\lambda) = 0, \tag{47}$$

$$\alpha_0(\lambda) = 0, \tag{48}$$

$$\lim_{x\to 0} \{\Theta, \Phi, \alpha_0\} = 0, \tag{49}$$

where $\Theta = -w'$, $\Phi = f'$ and $\alpha_0$ refers to the axisymmetric behavior. The conditions (49) follow from symmetry and boundedness of the membrane forces at the apex.

*Average deflection parameter*

As a suitable non-dimensional measure of the deflection of the cap under a given axisymmetric load, the ratio of the average vertical displacement of the region $r \leq \bar{r}$ to the weighted thickness parameter $t^*$ is selected where $\bar{r} = r_0$ for the ring load and $\bar{r} = r_2$ for the band load. Accordingly,

$$\frac{\overline{W}}{t^*} \equiv \frac{1}{\pi \bar{r}^2 t^*} \int_0^{2\pi} \mathrm{d}\varphi \int_0^{\bar{r}} rW\,\mathrm{d}r. \tag{50}$$

When the deformations are axisymmetrical, equation (50) reduces to

$$\frac{\overline{W}}{t^*} \equiv \frac{1}{[12(1-\nu^2)]^{\frac{1}{4}}} \int_0^{\lambda} y\Theta\,\mathrm{d}x \tag{51}$$

where

$$y = \begin{cases} \dfrac{x^2}{\bar{x}^2} & x < \bar{x} \\ 1 & x \geq \bar{x}, \end{cases} \tag{52}$$

and

$$\bar{x} = \begin{cases} x_0 \text{ (for the ring load)} \\ x_2 \text{ (for the band load).} \end{cases}$$

Defining $S_0$ as the rate of change of the load parameter $p$ with respect to the gross deflection parameter $\overline{W}/t^*$ at $p_c$ for the axisymmetrical path there results

$$\frac{1}{S_0} \equiv \frac{\mathrm{d}}{\mathrm{d}p}\left(\frac{\overline{W}}{t^*}\right) = \frac{1}{[12(1-\nu^2)]^{\frac{1}{4}}} \int_0^{\lambda} y\left(\frac{\partial \Theta}{\partial p}\right)_c \mathrm{d}x \tag{53}$$

where $(\partial\Theta/\partial p)_c$ is to be evaluated at the bifurcation point.

*Buckling equations*

In order to determine if asymmetric buckling precedes axisymmetrical buckling a solution of equations (27)–(36) is sought in the form

$$\begin{Bmatrix} w \\ f \\ \bar{\alpha} \\ \bar{\beta} \end{Bmatrix} = \begin{Bmatrix} \int_x^{\lambda} \Theta\,\mathrm{d}x \\ \int_0^{x} \Phi\,\mathrm{d}x \\ \alpha_0 \\ 0 \end{Bmatrix} + \xi \begin{Bmatrix} w_1(x,\varphi) \\ f_1(x,\varphi) \\ \alpha_1(x,\varphi) \\ \beta_1(x,\varphi) \end{Bmatrix} \tag{54}$$

where $\xi$ is an infinitesimal scalar parameter. Substituting expressions (54) into equations (27)–(36), making use of equations (43)–(48), and linearizing with respect to $\xi$, there is obtained the system of differential equations

$$\nabla^4 w_1 = \nabla^2 f_1 - \frac{1}{x} f_1''\Theta + \left(\frac{1}{x^2}\ddot{w}_1 + \frac{1}{x}w_1'\right)\Phi' + \frac{1}{x}w_1''\Phi - \left(\frac{1}{x}f_1' + \frac{1}{x^2}\ddot{f}_1\right)\Theta'$$

$$-\eta\left(\alpha_1' + \frac{1}{x}\alpha_1 + \frac{1}{x}\dot{\beta}_1 - \nabla^2 w_1\right), \tag{55}$$

$$\nabla^4 f_1 = -\nabla^2 w_1 + \frac{1}{x}w_1''\Theta + \left(\frac{1}{x}w_1' + \frac{1}{x^2}\ddot{w}_1\right)\Theta', \tag{56}$$

$$\frac{1-\nu}{2}\nabla^2\alpha_1 + \frac{1+\nu}{2}\left(\alpha_1'' + \frac{1}{x}\alpha_1' + \frac{1}{x}\dot{\beta}_1'\right) - \frac{1}{x^2}\alpha_1 - \frac{3-\nu}{2x^2}\dot{\beta}_1 - \Lambda(\alpha_1 - w_1') = 0, \tag{57}$$

$$\frac{1-\nu}{2}\nabla^2\beta_1 + \frac{1+\nu}{2}\left(\frac{1}{x}\dot{\alpha}_1' + \frac{1}{x^2}\ddot{\beta}_1\right) + \frac{3-\nu}{2x^2}\dot{\alpha}_1 - \frac{1-\nu}{2x^2}\beta_1 - \Lambda\left(\beta_1 - \frac{1}{x}\dot{w}_1\right) = 0, \tag{58}$$

with boundary conditions at the clamped edge ($x = \lambda$)

$$w_1 = 0 \tag{59}$$

$$w_1' = 0, \tag{60}$$

$$f_1'' - \frac{\nu}{\lambda}f_1' - \frac{\nu}{\lambda^2}\ddot{f}_1 = 0, \tag{61}$$

$$\lambda\left(f_1'' - \frac{\nu}{x}f_1' - \frac{\nu}{x^2}\ddot{f}_1\right)' - \frac{1}{\lambda}f_1' - \frac{1}{\lambda^2}\ddot{f}_1 + \nu f_1'' + 2(1+\nu)\left(\frac{1}{x}\ddot{f}_1\right)' = 0, \tag{62}$$

$$\alpha_1 = 0, \tag{63}$$

$$\beta_1 = 0. \tag{64}$$

Equations (55)–(64), along with suitable regularity conditions at the apex, constitute a linear eigenvalue problem in which the loading parameter $p$ occurs implicitly through the function $\Theta$ and $\Phi$.

Taking

$$\left.\begin{aligned} w_1(x,\varphi) &= w_{1n}(x)\cos n\varphi, \\ f_1(x,\varphi) &= f_{1n}(x)\cos n\varphi, \\ \alpha_1(x,\varphi) &= \alpha_{1n}(x)\cos n\varphi, \\ \beta_1(x,\varphi) &= \beta_{1n}(x)\sin n\varphi, \end{aligned}\right\} \tag{65}$$

equations (55)–(64) yield the system of homogeneous equations

$$L_n^2(w_{1n}) = L_n(f_{1n}) - \left(\frac{1}{x}f'_{1n} - \frac{n^2}{x^2}f_{1n}\right)\Theta' + \frac{1}{x}w''_{1n}\Phi - \frac{1}{x}f''_{1n}\Theta$$

$$+\left(\frac{1}{x}w'_{1n} - \frac{n^2}{x^2}w_{1n}\right)\Phi' - \eta\left[\alpha'_{1n} + \frac{1}{x}\alpha_{1n} + \frac{n}{x}\beta_{1n} - L_n(w_{1n})\right], \tag{66}$$

$$L_n^2(f_{1n}) = -L_n(w_{1n}) + \left(\frac{1}{x}w'_{1n} - \frac{n^2}{x^2}w_{1n}\right)\Theta' + \frac{1}{x}w''_{1n}\Theta, \tag{67}$$

$$\frac{1-\nu}{2}L_n(\alpha_{1n}) + \frac{1+\nu}{2}\left(\alpha''_{1n} + \frac{1}{x}\alpha'_{1n} + \frac{n}{x}\beta'_{1n}\right) - \frac{1}{x^2}\alpha_{1n} - \frac{(3-\nu)n}{2x^2}\beta_{1n} - \Lambda(\alpha_{1n} - w'_{1n}) = 0, \tag{68}$$

$$\frac{1-\nu}{2}L_n(\beta_{1n}) + \frac{1+\nu}{2}\left(-\frac{n}{x}\alpha'_{1n} - \frac{n^2}{x^2}\beta_{1n}\right) - \frac{(3-\nu)n}{2x^2}\alpha_{1n} - \frac{1-\nu}{2x^2}\beta_{1n} - \Lambda\left(\beta_{1n} + \frac{n}{x}w_{1n}\right) = 0, \tag{69}$$

and boundary conditions at the clamped edge ($x = \lambda$)

$$w_{1n} = 0, \tag{70}$$

$$w'_{1n} = 0, \tag{71}$$

$$f''_{1n} - \frac{\nu}{\lambda}f'_{1n} + \frac{\nu n^2}{\lambda^2}f_{1n} = 0, \tag{72}$$

$$\lambda f'''_{1n} - \frac{1}{\lambda}[(1-\nu) + n^2(2+\nu)]f'_{1n} + \frac{3n^2}{\lambda^2}f_{1n} = 0, \tag{73}$$

$$\alpha_{1n} = 0, \tag{74}$$

$$\beta_{1n} = 0. \tag{75}$$

The differential operators appearing in these relations are defined by

$$L_n(\ ) \equiv (\ )'' + \frac{1}{x}(\ )' - \frac{n^2}{x^2}(\ ), \qquad L_n^2(\ ) \equiv L_nL_n(\ ).$$

To the system of equations (66)–(75) there are added the conditions of regularity at the apex

$$\lim_{x\to 0}\{w_{1n}, xw''_{1n}, f_{1n}, xf''_{1n}, \alpha_{1n}, \beta_{1n}\} = 0. \tag{76}$$

The critical bifurcation pressure $p_c$ is the lowest value of $p$ for which equations (66)–(76) possess a non-trivial solution for any integer $n$.

*Initial post-buckling behavior*

In order to investigate the initial post-buckling behavior of the clamped shallow spherical sandwich cap under the axisymmetrical loads described earlier the nondimensional transverse deflection, Airy stress functions and transverse shear angles are assumed to have the forms

$$\left.\begin{aligned} w &= -\int^{x} \Theta \, dx + \xi w_1 + \xi^2 w_2(x, \varphi) + \ldots, \\ f &= \int_0^{x} \Phi \, dx + \xi f_1 + \xi^2 f_2(x, \varphi) + \ldots, \\ \bar{\alpha} &= \alpha_0 + \xi \alpha_1 + \xi^2 \alpha_2(x, \varphi) + \ldots, \\ \bar{\beta} &= \beta_0 + \xi \beta_1 + \xi^2 \beta_2(x, \varphi) + \ldots, \end{aligned}\right\} \tag{77}$$

for a slightly buckled configuration. Here $\xi$ is an infinitesimal scalar parameter. The function $\beta_0(x) \equiv 0$ by symmetry. Substituting the relations (77) into the general nonlinear equations (27)–(36), observing that at the bifurcation point both the systems of equations (43)–(49) and (55)–(64) hold, and letting $\xi \to 0$ yields the system of equations

$$\begin{aligned} &\nabla^4 w_2 - \nabla^2 f_2 + \left(\frac{1}{x} f'_2 + \frac{1}{x^2} \ddot{f}_2\right)\Theta'_c - \frac{1}{x} w''_2 \Phi_c + \frac{1}{x} f''_2 \Theta_c - \left(\frac{1}{x} w'_2 + \frac{1}{x^2} \ddot{w}_2\right)\Phi'_c \\ &\quad + \eta\left(\alpha'_2 + \frac{1}{x}\alpha_2 + \frac{1}{x}\dot{\beta}_2 - \nabla^2 w_2\right) = \left(\frac{1}{x} f'_1 + \frac{1}{x^2}\ddot{f}_1\right) w''_1 + \left(\frac{1}{x} w'_1 + \frac{1}{x^2}\ddot{w}_1\right) f''_1 \\ &\quad - 2\left(\frac{1}{x^2}\dot{f}_1 - \frac{1}{x}\dot{f}'_1\right)\left(\frac{1}{x^2}\dot{w}_1 - \frac{1}{x}\dot{w}'_1\right), \end{aligned} \tag{78}$$

$$\nabla^4 f_2 + \nabla^2 w_2 - \left(\frac{1}{x^2}\ddot{w}_2 + \frac{1}{x} w'_2\right)\Theta'_c - \frac{1}{x} w''_2 \Theta_c = \left(\frac{1}{x}\dot{w}'_1 - \frac{1}{x^2}\dot{w}_1\right)^2 - \left(\frac{1}{x^2}\ddot{w}_1 + \frac{1}{x} w'_1\right) w''_1, \tag{79}$$

$$\frac{1-\nu}{2}\nabla^2 \alpha_2 + \frac{1+\nu}{2}\left(\alpha''_2 + \frac{1}{x}\alpha'_2 + \frac{1}{x}\dot{\beta}'_2\right) - \frac{1}{x^2}\alpha_2 - \frac{3-\nu}{2x^2}\dot{\beta}_2 - \Lambda(\alpha_2 - w'_2) = 0, \tag{80}$$

$$\frac{1-\nu}{2}\nabla^2 \beta_2 + \frac{1+\nu}{2}\left(\frac{1}{x}\dot{\alpha}'_2 + \frac{1}{x^2}\ddot{\beta}_2\right) + \frac{3-\nu}{2x^2}\dot{\alpha}_2 - \frac{1-\nu}{2x^2}\beta_2 - \Lambda\left(\beta_2 - \frac{1}{x}\dot{w}_2\right) = 0, \tag{81}$$

and boundary conditions (31)–(36) on $w_2, f_2, \alpha_2$ and $\beta_2$.

It can be shown by direct substitution into equations (78)–(81) and the associated boundary conditions at $x = \lambda$ and conditions of regularity at $x = 0$ that the functions $w_2, f_2, \alpha_2, \beta_2$ must be of the form

$$\left.\begin{aligned} w_2(x, \varphi) &= -\int^{x} \zeta(x) \, dx + \rho(x) \cos 2n\varphi, \\ f_2(x, \varphi) &= \int^{x} \psi(x) \, dx + \chi(x) \cos 2n\varphi, \\ \alpha_2(x, \varphi) &= \gamma(x) + \sigma(x) \cos 2n\varphi, \\ \beta_2(x, \varphi) &= \omega(x) + \tau(x) \sin 2n\varphi, \end{aligned}\right\} \tag{82}$$

where $\zeta(x)$, $\psi(x)$ and $\gamma(x)$ must satisfy the boundary value problem

$$(x\zeta')' - \left(\frac{1}{x} + \Phi_c\right)\zeta + (x - \Theta_c)\psi - \eta x(\gamma + \zeta) = g_1(x), \tag{83}$$

$$(x\psi')' - \frac{1}{x}\psi - (x - \Theta_c)\zeta = g_2(x), \tag{84}$$

$$L_1(\gamma) - \Lambda(\gamma + \zeta) = 0, \tag{85}$$

$$\zeta(\lambda) = 0, \tag{86}$$

$$\lambda\psi'(\lambda) - \nu\psi(\lambda) = 0, \tag{87}$$

$$\gamma(\lambda) = 0, \tag{88}$$

$$\lim_{x \to 0} \{\zeta, \psi, \gamma\} = 0, \tag{89}$$

and the functions $\rho(x)$, $\chi(x)$, $\sigma(x)$ and $\tau(x)$ must satisfy the boundary value problem

$$L_{2n}^2(\rho) - L_{2n}(\chi) + \left(\frac{1}{x}\chi' - \frac{4n^2}{x^2}\chi\right)\Theta_c' - \left(\frac{1}{x}\rho' - \frac{4n^2}{x^2}\rho\right)\Phi_c'$$
$$- \frac{1}{x}\rho''\Phi_c + \frac{1}{x}\chi''\Theta_c + \eta\left[\frac{1}{x}(x\sigma)' + \frac{2n}{x}\tau - L_{2n}(\rho)\right] = h_1(x), \tag{90}$$

$$L_{2n}^2(\chi) + L_{2n}(\rho) - \left(\frac{1}{x}\rho' - \frac{4n^2}{x^2}\rho\right)\Theta_c' - \frac{1}{x}\rho''\Theta_c = h_2(x), \tag{91}$$

$$\frac{1-\nu}{2}L_{2n}(\sigma) + \frac{1+\nu}{2}\left(\sigma'' + \frac{1}{x}\sigma' + \frac{2n}{x}\tau'\right) - \frac{1}{x^2}\sigma - \frac{(3-\nu)n}{x^2}\tau - \Lambda(\sigma - \rho') = 0, \tag{92}$$

$$\frac{1-\nu}{2}L_{2n}(\tau) + \frac{1+\nu}{2}\left(-\frac{2n}{x}\sigma' - \frac{4n^2}{x^2}\tau\right) - \frac{(3-\nu)n}{x^2}\sigma - \frac{1-\nu}{2x^2}\tau - \Lambda\left(\tau + \frac{2n}{x}\rho\right) = 0, \tag{93}$$

$$\rho(\lambda) = 0, \tag{94}$$

$$\rho'(\lambda) = 0, \tag{95}$$

$$\chi''(\lambda) - \frac{\nu}{\lambda}\chi'(\lambda) + \frac{4n^2\nu}{\lambda^2}\chi(\lambda) = 0, \tag{96}$$

$$\lambda\chi'''(\lambda) - \frac{1}{\lambda}[(1-\nu) + 4(2+\nu)n^2]\chi'(\lambda) + \frac{12n^2}{\lambda^2}\chi(\lambda) = 0, \tag{97}$$

$$\sigma(\lambda) = 0, \tag{98}$$

$$\tau(\lambda) = 0, \tag{99}$$

$$\lim_{x \to 0} \{\rho, \chi, x\rho'', x\chi'', \sigma, \tau\} = 0. \tag{100}$$

The boundary value problem for the function $\omega(x)$ is

$$\frac{1-\nu}{2}L_1(\omega)-\Lambda\omega = 0, \tag{101}$$

$$\omega(\lambda) = 0, \tag{102}$$

$$\lim_{x\to 0}\{\omega\} = 0, \tag{103}$$

and yields $\omega \equiv 0$.

The functions on the right-hand sides of equations (83), (84), (90) and (91) are defined by the relations

$$g_1(x) = \frac{1}{2}\left[n^2\left(\frac{w_{1n}f_{1n}}{x}\right)' - f'_{1n}w'_{1n}\right], \tag{104}$$

$$g_2(x) = \frac{1}{4}\left[n^2\left(\frac{w_{1n}^2}{x}\right)' - (w'_{1n})^2\right], \tag{105}$$

$$h_1(x) = \frac{1}{2}\left[\left(\frac{1}{x}f'_{1n} - \frac{n^2}{x^2}f_{1n}\right)w''_{1n} + \left(\frac{1}{x}w'_{1n} - \frac{n^2}{x^2}w_{1n}\right)f''_{1n} + 2n^2\left(-\frac{1}{x^2}f_{1n} + \frac{1}{x}f'_{1n}\right)\right.$$
$$\left.\times\left(-\frac{1}{x^2}w_{1n} + \frac{1}{x}w'_{1n}\right)\right], \tag{106}$$

$$h_2(x) = -\frac{1}{2}\left[\left(\frac{1}{x}w'_{1n} - \frac{n^2}{x^2}w_{1n}\right)w''_{1n} + n^2\left(\frac{1}{x^2}w_{1n} - \frac{1}{x}w'_{1n}\right)^2\right]. \tag{107}$$

These formulas are precisely the same as those encountered for the homogeneous spherical cap [2, 4–6].

It is shown in Ref. [2] that the expansions (77), when they are assumed asymptotically valid for $\xi \ll 1$, imply a relationship of the form

$$\frac{p}{p_c} = 1 + a\xi + b\xi^2 + \ldots, \tag{108}$$

It can be shown that the coefficients $a \equiv 0$ for the spherical sandwich cap and

$$b = -\frac{1}{p_c}\frac{\int_0^\lambda[(\zeta g_1 - \psi g_2) - \frac{1}{2}x(\rho h_1 - \chi h_2)]\,\mathrm{d}x}{\displaystyle\int_0^\lambda\left[g_1\left(\frac{\partial\Theta}{\partial p}\right)_c - g_2\left(\frac{\partial\Phi}{\partial p}\right)_c\right]\mathrm{d}x}. \tag{109}$$

By using the definitions (104) and (105) and equations obtained by differentiating the axisymmetrical equilibrium equations (43)–(45) with respect to the load parameter $p$, the integral in the denominator of equation (109) can be written in the more convenient form

$$\left.\begin{aligned} &-\int_0^\lambda h(x-x_0)\zeta\,\mathrm{d}x, && \text{(ring load)} \\ &-2(x_2^2-x_1^2)\int_0^\lambda Z(x)\zeta\,\mathrm{d}x, && \text{(band load).} \end{aligned}\right\} \tag{110}$$

The sign of the coefficient $b$ determines whether the load initially increases or decreases subsequent to asymmetrical buckling. The significance of the coefficient $b$ is connected with the notions of imperfection-sensitive and imperfection-insensitive structures. It has been shown in Refs. [2, 4] that structures containing geometric imperfections (imperfect structures) are imperfection-sensitive, in the sense that the buckling load for the imperfect structure should be expected to be less than that for the corresponding perfect structure, whenever the load for the perfect structure initially decreases at the bifurcation point. A structure is said to be imperfection-insensitive, in the sense that load–deflection curve for the imperfect structure exhibits a much milder growth of displacement as the load reaches and exceeds the classical buckling load of the corresponding perfect structure, whenever the load for the perfect structure increases subsequent to asymmetrical buckling. Accordingly, a structure is said to be imperfection-sensitive or imperfection-insensitive according to whether $b$ is negative or positive, respectively. In calculating $b$ it has been assumed that the buckling mode $(w_1, f_1)$ has been normalized so that the maximum value of $W_1(=2H/\lambda^2 w_1)$ is equal to the weighted shell thickness $(t^*)$.

Let $S$ represent the initial slope of the load–deflection curve corresponding to the bifurcation path. It is not difficult to show that

$$S = \frac{S_0}{1+\delta} \tag{111}$$

where

$$\delta = \frac{S_0}{bp_c[12(1-\nu^2)]^{\frac{1}{2}}} \int_0^\lambda y\zeta \, \mathrm{d}x. \tag{112}$$

The function $\zeta(x)$ is defined by the boundary value problem (83)–(89), $b$ is the initial post-buckling coefficient defined by equation (109) and $p_c$ is the value of the loading parameter $p$ at the bifurcation point.

Finally, as a measure of the relative stiffness the following parameter is used.

$$\vartheta = \frac{2}{\pi} \arctan \frac{1}{\delta}. \tag{113}$$

The parameters $S_0$, $S$ and $\vartheta$ were defined by Fitch and Budiansky [4] and the average deflection parameter defined here is analogous to the one defined by those authors. The parameter $\vartheta$ can vary between $+1$ and $-1$, and it is positive for increasing load, and negative for decreasing load (Fig. 4). Values of $\vartheta$ between $-1$ and $-\frac{1}{2}$ correspond to a backward sloping post-buckling load–deflection curve, with decreasing load.

## NUMERICAL RESULTS AND CONCLUSIONS

The numerical results presented in this paper are for a clamped shallow spherical sandwich shell with equal face sheets for which the pertinent geometric and material parameters are $c/t = 10$, $(G_c/E)(a/H)^2 = 0{\cdot}8$ and $\nu = \frac{1}{3}$ and which is subjected to a uniform pressure distributed over the entire surface of the shell.

The numerical procedures employed in this study have been described in detail by Fitch [2]. A brief account of our application of these procedures is presented here to provide a clearer understanding of the numerical results to be presented in the sequel.

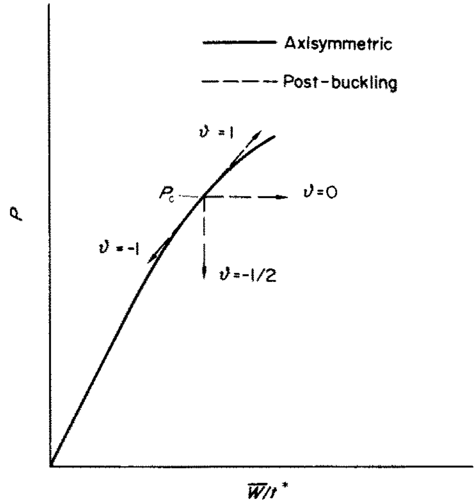


FIG. 4. Interpretation of relative stiffness parameter $\vartheta$.

The system of nonlinear differential equations (43)–(49) governing the axisymmetrical buckling of the sandwich cap was solved by Newton's method, which, essentially, replaces these equations with a system of linear correctional equations. This latter system of equations was in turn approximated by a system of finite difference equations using central difference formulas for the derivatives. The linear correctional equations lead, via an iterative process, to the solution of the axisymmetrical problem. The numerical procedure employed was to solve the linearized finite difference analogue of the axisymmetrical equations (43)–(49) for a value of $p$ (in the present case $p = 0{\cdot}5$) for which the shell response was linear and to use this solution as an initial estimate of the solution for a slightly higher value of $p$. The finite difference analogue of the linear correctional equations was solved then by an iterative process for the correction functions associated with these initial estimates of the solution. It was found that convergence of the iterative process occurred after an average of 3–4 iterations when $p$ was incremented in steps of 2·0. The correction functions were considered to be sufficiently accurate whenever their absolute values at each station were less than 0·01 per cent of the absolute values of the current estimate of the solution at the corresponding station. Having obtained the solution for a given value of $p$ it was used as an initial estimate for a slightly higher value of $p$ and the process was continued until convergence did not occur.

Axisymmetrical cap-snapping was assumed to occur when a local maximum on the axisymmetrical load–deflection curve was reached. The occurrence of a local maximum was signified by the failure of the iterative process to converge. In locating the local maximum numerically it was assumed that it has been exceeded if convergence of the system of linear correctional equations has not occurred after fourteen iterations for a fixed value of the loading parameter $p$. The preceding value of $p$ for which convergence had occurred was then incremented in steps of 0·2 ($\frac{1}{10}$ of the original increment) until convergence, in the sense described, failed to occur. This latter process was repeated for increments 0·02 ($\frac{1}{100}$ of the original increment) until convergence failed to occur. The immediately preceding value of $p$ was taken as the axisymmetrical buckling load. This process gives the critical axisymmetrical buckling load to two places after the decimal point.

The linear eigenvalue problem, equations (66)–(76), describing the asymmetrical buckling of the shallow sandwich cap was replaced with a finite difference analogue using central difference formulas. Potters' algorithm [9], with the modifications suggested by Blum and Fulton [10] which eliminate sign changes associated with the singularities of the buckling determinant, was used in determining the asymmetrical buckling load. The value of the modified buckling determinant was plotted against the corresponding value of the load parameter $p$ for several values of the circumferential wave number $n$. Whenever a change in sign of the modified buckling determinant occurred the preceding value of $p$ was incremented in steps of 0·2 and the process was repeated until the sign change was detected again. The asymmetrical buckling load was taken as the value of $p$ corresponding to a linear interpolation between the value of $p$ immediately preceding the sign change for the refined calculations and the value of $p$ associated with the sign change.

The initial post-buckling problem, equations (83)–(89) and (90)–(100), was replaced by a finite difference analogue using central difference formulas. Potters' algorithm was used to generate the solution. The integrals appearing in the numerator and denominator of the initial post-buckling coefficient $b$ [equation (109)] and in the formula for the relative stiffness parameter $\vartheta$ [equation (113)] were evaluated by Simpson's rule.

The preceding calculations were carried out for a mesh size of 0·5 on the IBM 360-50 computer using double precision throughout. A mesh size of 0·25 was used at two points so as to ascertain the accuracy with which the buckling loads and associated mode forms were given by the 0·5 mesh. The buckling loads associated with the 0·5 mesh were found to be less than 1 per cent larger than those associated with the 0·25 mesh. Moreover, the initial post-buckling coefficient ($b$) and the relative stiffness parameter ($\vartheta$) differed by approximately 2 and 4 per cent, respectively. These differences were not considered to be significant since the important information extracted from the plots did not change. Consequently, the 0·5 mesh was used throughout the study.

Figure 5 shows the buckling and initial post-buckling behavior of a clamped shallow spherical sandwich cap under a uniform pressure distributed over its entire surface. The upper plot gives the critical value of the load parameter $p$ as a function of the geometric parameter $\lambda$. The intermediate and lower plots give the initial post-buckling coefficient $b$ and the relative stiffness parameter $\vartheta$ as functions of the geometric parameter $\lambda$.

The qualitative description of the buckling and initial post-buckling behavior for the clamped shallow spherical sandwich cap under a uniform pressure over its entire surface is precisely the same as for the clamped homogeneous cap under the same load [3]. For $14 \leq \lambda < 24$ the buckling behavior is of the axisymmetrical type. For $\lambda \geq 24$ the buckling behavior is of the asymmetrical type with $b < 0$ which signifies that the asymmetrical buckling process is characterized by a decrease in load carrying capacity for this range of $\lambda$. Consequently, for $14 \leq \lambda$ the buckling process is characterized by a snap-through type of behavior. Since the relative stiffness parameter $\vartheta < 0{\cdot}5$ for $\lambda \geq 24$ it follows that a decrease in deflection accompanies the decrease in load, i.e. the initial slope of the bifurcation branch of the load–deflection curve is backward.

It was observed, for $\lambda < 14$, that snap-through buckling did not occur. Instead, the deflection of the cap was characterized by a gradual transition from one equilibrium state to another. In most cases an inflection point type of behavior was observed, as shown in Fig. 6, for $\lambda < 14$. This behavior has also been reported by Huang [3] for the homogeneous cap.

Figure 7 indicates some typical asymmetrical buckling mode shapes. Again, the general shapes and the locations of the peak asymmetrical deflections are very nearly the same for

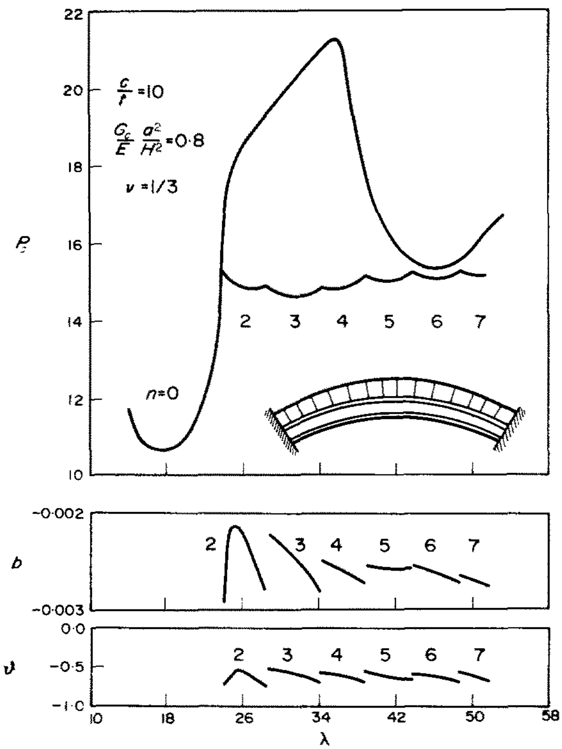


FIG. 5. Buckling and initial post-buckling behavior of clamped shallow sandwich spherical shells under uniform pressure.

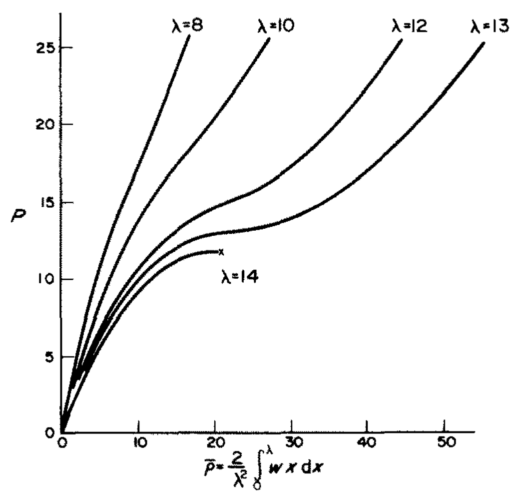


FIG. 6. Nondimensional axisymmetrical load deflection curves for clamped shallow sandwich spherical shells under uniform pressure.

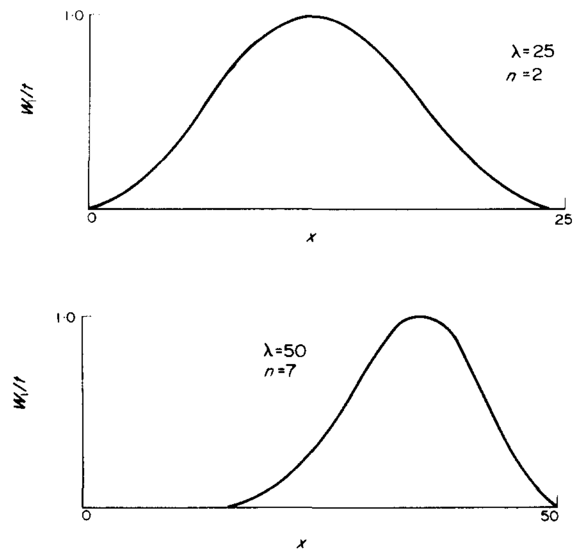


FIG. 7. Buckling mode shapes for $\lambda = 25$ and $\lambda = 50$.

both the homogeneous and sandwich caps [3]. A last interesting observation is that the asymmetrical buckling curve of Fig. 5 can be obtained directly from the plot given by Huang [3] by means of the relations

$$(\lambda)_S = 4{\cdot}3(\lambda)_H, \tag{114}$$

and

$$(p_c)_S = 19{\cdot}1(p_c)_H, \tag{115}$$

where the subscripts $S$ and $H$ correspond to sandwich and homogeneous shells, respectively.

*Acknowledgement*—The financial support for this investigation was provided by the Department of Engineering Mechanics of Clemson University.

## REFERENCES

[1] W. T. KOITER, Elastic Stability and Post-Buckling Behavior, *Proc. Symp. Nonlinear Problems*, edited by R. E. LANGER, p. 257. University of Wisconsin Press (1963).
[2] J. R. FITCH, The buckling and post-buckling behavior of spherical caps under concentrated load. *Int. J. Solids Struct.* **4**, 421 (1968).
[3] N. C. HUANG, Unsymmetrical buckling of thin shallow spherical shells. *J. appl. Mech.* **31**, 447 (1964).
[4] J. R. FITCH and B. BUDIANSKY, Buckling and post-buckling behavior of spherical caps under axisymmetric load. *AIAA Jnl* **8**, 686 (1970).
[5] N. AKKAŞ and N. R. BAULD, JR., Buckling and post-buckling behavior of clamped shallow spherical shells under axisymmetric ring loads. *J. appl. Mech.* to be published.
[6] N. AKKAŞ and N. R. BAULD, JR., Buckling and Initial Post-Buckling Behavior of Clamped Shallow spherical Shells under Axisymmetric Band Type Loads, XIV *South American Sessions on Structural Engineering and* IV *Symposium on Pan American Structures*, Buenos Aires, Argentina (1970).
[7] J. F. MESCALL, Large Deflections of Spherical Shells Under Concentrated, Distributed and Ring Loadings, *Developments in Theoretical and Applied Mechanics*, edited by D. FREDERICK, Vol. 4, p. 183. Pergamon Press (1970).

[8] D. BUSHNELL, Bifurcation phenomena in spherical shells under concentrated and ring loads. *AIAA Jnl* **5**, 2034 (1967).
[9] M. L. POTTERS, A Matrix Method for the Solution of a Second Order Difference Equation in Two Variables, Report MR 19, Mathematich Centrum, Amsterdam, Holland (1955).
[10] R. E. BLUM and R. E. FULTON, A modification of Potters' method for solving eigenvalue problems involving tridiagonal matrices. *AIAA Jnl* **4**, 2231 (1966).

(*Received* 22 *September* 1970; *revised* 9 *December* 1970)

**Абстракт**—В работе дается разработка системы нелинейных дифференциальных уравнений, пригодных для анализа выпучивания и начального поведения после потери устойчивости тонких, пологих, сферических, сандвичевых оболочек, под влиянием осесимметрической нагрузки. Решаются также краевые задачи, связанные с осесимметрическим поведением, антисимметрическим и начальным поведением после потери устойчивости для защемленных, пологих, сферических, сандвичевых оболочек, под влиянием некоторых осесимметрических нагрузок. В конце концов, исследуется численные результаты поведения выпучивания и начального поведения после потери устойчивости для защемленных, пологих, сферических, сандвичевых оболочек, подверженных давлению, распределенному равномерно по целой о относительной поверхности оболочки. Исследования касаются поверхностных листов из того же материала и равной толщины. Численные результаты указывают, что выпучивание и иачальное поведение после потери устойчивости для сандвичевого колпака очень подобно.